JVI Journals.ASM.org

Spatiotemporal Dynamics of Adenovirus Membrane Rupture and Endosomal Escape

Oana Maier,[a] Shauna A. Marvin,[a] Harald Wodrich,[b] Edward M. Campbell,[a] and Christopher M. Wiethoff[a]

Department of Microbiology and Immunology, Loyola University Chicago Stritch School of Medicine, Maywood, Illinois, USA,[a] and Laboratoire de Microbiologie Fondamental et Pathogénicité, MFP CNRS UMR 5234, Université de Bordeaux 2, Bordeaux, France[b]

A key step in adenovirus cell entry is viral penetration of cellular membranes to gain access to the cytoplasm and deliver the genome to the nucleus. Yet little is known about this important event in the adenoviral life cycle. Using the cytosolic protein galectin-3 (gal3) as a marker of membrane rupture with both live- and fixed-cell imaging, we demonstrate that in the majority of instances, exposure of pVI and recruitment of gal3 to ruptured membranes occur early at or near the cell surface and occur minimally in EEA-1-positive (EEA-1$^+$) early endosomes or LAMP-1$^+$ late endosomes/lysosomes. Live-cell imaging of Ad5 egress from gal3$^+$ endosomes occurs most frequently from perinuclear locations. While the Ad5 capsid is observed escaping from gal3$^+$ endosomes, pVI appears to remain associated with the gal3$^+$ ruptured endosomes. Thus, Ad5 membrane rupture and endosomal escape appear to be both spatially and temporally distinct events.

Adenoviruses (Ads) have evolved a seemingly complex mechanism to efficiently deliver their double-stranded DNA (dsDNA) genome to the nucleus. This mechanism appears to be highly processive, involving multiple viral-host interactions (29). A key to Ad cell entry is the stepwise disassembly of the virion as it traffics from the cell surface to the nuclear envelope (15). A lack of specific cellular markers encountered along this entry route has made identifying specific subcellular locations for Ad uncoating difficult.

While uncoating of species C Ads was initially proposed to occur in acidified endosomes (15), more recent observations suggest that mechanical disassembly of the capsid may be initiated at, or very near, the cell surface (6, 34). This event appears to involve movement of the relatively motile coxsackievirus and adenovirus receptor (CAR) bound to the Ad fiber protein away from relatively immobile alpha$_v$ integrins, which bind to the Ad penton base (6). Uncoating at the cell surface was also recently found to result in the exposure of membrane lytic protein VI (pVI) from the capsid interior (6, 34). Uncoating of Ads and release of pVI are necessary to penetrate cell membranes, allowing the virus access to the cytoplasm (33).

Engagement of alpha$_v$ integrins by species C Ads also induces clathrin-mediated endocytosis of virions (24, 29). The virus then traffics within endosomal compartments, although a clear description of markers associated with species C Ad endosomal trafficking is lacking. While disruption of molecules associated with early endosomal compartments by RNA interference or expression of dominant-negative proteins suggests that adenovirus traffics through early endosomal compartments, evidence of colocalization of incoming Ad virions with markers of early endosomes during synchronous infections is meager (12, 22).

Rupture of endosomes by pVI released from the Ad capsid interior ultimately allows the virus access to the cytoplasm (33). Considerable biochemical and biophysical evidence suggests that pVI fragments membranes by inducing positive membrane curvature stress (20). These *in vitro* observations of the mechanism of pVI membrane rupture are supported by the observation that Ad infection facilitates cytosolic translocation of coendocytosed high-molecular-mass molecules, such as 70-kDa dextrans or whole parvoviruses, in cell culture (9, 26). This suggests that Ad rupture of endosomes is catastrophic, resulting in the release of Ads and endosomal contents into the cytoplasm. This endosomal rupture was recently demonstrated to serve as a danger signal which activates an innate proinflammatory response (2, 3, 21).

Upon entering the cytoplasm, species C Ads then traffic to the nucleus via microtubules (15). Interactions between the hexon and dynein intermediate light chains are thought to mediate plus-end microtubule movement of the partially disassembled virions (5). Upon docking at the nuclear pore complex, via interactions with Nup214 and Nup358, kinesin binding to Ad capsid protein IX and Nup358 results in further disassembly of the species C capsid, releasing the viral genome and allowing it to be translocated into the nucleus (30).

A major limitation to studies of Ad trafficking during cell entry is the inability to specifically define where and when these events occur, in part due to the lack of reliable markers to distinguish between Ad trafficking within endosomes and in the cytoplasm. Limited data about Ad membrane rupture have been provided by studies using membrane-impermeative toxins (α-sarcin) to quantify the relative amount of Ad-induced membrane rupture or transmission electron microscopy (TEM) to determine the amount of Ad in the cytoplasm compared to endosomes (17, 22, 34). Recently, Paz et al. identified the cytosolic protein galectin-3 (gal3) as a marker for bacterially ruptured phagosome membranes (25). gal3, a member of the galectin family, contains a consensus sequence in its carbohydrate binding domain (CRD), which has affinity for β-galactoside-containing glycoconjugates (4, 16, 19). The cytosolic gal3 is recruited to disrupted membranes by binding

Received 8 June 2012 **Accepted** 23 July 2012
Published ahead of print 1 August 2012
Address correspondence to Christopher M. Wiethoff, cwiethoff@lumc.edu.
O. Maier and S. A. Marvin contributed equally to this article.
Supplemental material for this article may be found at http://jvi.asm.org/.

doi:10.1128/JVI.01428-12

N-linked glycans found on the exterior surface of the plasma membrane when they are exposed from the interior vacuole surface following lysis (25).

In agreement with a model of gross membrane reorganization during Ad endosomal escape, we have determined that gal3 is recruited to Ad5-ruptured membranes. Using gal3 as a marker for Ad endosomal membrane rupture, we determined that release of pVI from the virus interior occurs within minutes of initiating a synchronous infection, at or near the cell surface. gal3 recruitment to Ad5-ruptured membranes is rapid and is frequently observed at or near the cell surface. Egress of Ad5 from ruptured endosomes occurs primarily from a perinuclear location, however. Exposure of pVI and recruitment of gal3 to Ad5-ruptured membranes occur at sites which do not strongly colocalize with conventional markers of early endosomes or late endosomes/lysosomes, suggesting Ad5 escape from an unknown endosomal compartment into the cytoplasm. Dissociation of the Ad virions, but not pVI, from these gal3-decorated membranes is observed, although the fate of the gal3-positive (gal3$^+$) pVI$^+$ membrane remnants is unknown. Together, these results demonstrate the utility of gal3 in dissecting the sequence of uncoating and trafficking events which occur during Ad cell entry.

MATERIALS AND METHODS

Cell lines and viruses. Tissue culture reagents were obtained from Mediatech and HyClone. U2OS and HeLa cells were obtained from ATCC, and 293β5 cells were a kind gift from Glen Nemerow (28). Cells were maintained in Dulbecco modified Eagle medium (DMEM) supplemented with 10% fetal bovine serum (FBS), 100 IU/ml penicillin, 1 mg/ml streptomycin, 0.25 μg/ml amphotericin B, nonessential amino acids, 1 mM sodium pyruvate, 10 mM HEPES buffer, and 2 mM glutamine. The temperature-sensitive mutant *ts1* (32) and Ad5gfp (33), an E1/E3-deleted adenovirus encoding enhanced green fluorescent protein (EGFP) under the control of a cytomegalovirus (CMV) promoter, were propagated in 293β5 cells. Viruses were purified from cellular lysates by double banding in cesium chloride gradients and dialyzed in 40 mM Tris–150 mM NaCl–10% glycerol–1 mM $MgCl_2$ (pH 8.2) (33). For these studies, the *ts1* virus was propagated at the nonpermissive temperature of 39.5°C (7, 14, 33). Viral concentrations were determined by a Bradford assay (Bio-Rad Laboratories, Inc.), and aliquots were flash frozen in liquid nitrogen and stored at −80°C. Reovirus strain T3D was derived from laboratory stocks which were twice plaque purified. Virus was propagated on L929 cells and purified by cesium chloride density gradient centrifugation as previously described (11).

Immunofluorescence microscopy. A total of 1×10^5 HeLa cells were plated on glass coverslips. The next day, the cells were infected with 3×10^4 virus particles (vp)/cell of Ad5gfp or *ts1* or with 3,000 PFU/cell of reovirus on ice for 1 h, after which the cells were shifted at 37°C to allow virus internalization. At different times post-virus internalization, the cells were washed with phosphate-buffered saline (PBS) and fixed with 4% paraformaldehyde (Electron Microscopy Sciences)–PBS or 3.7% paraformaldehyde–0.159 M PIPES [piperazine-*N*,*N*′-bis(2-ethanesulfonic acid)] buffer (Sigma) for 15 min. Cells were then blocked for 1 h in PBS with 10% FBS and 0.5% saponin (Sigma) or were then permeabilized with 0.5% (vol/vol) Triton X-100 (Sigma-Aldrich) for 2 min, washed with PBS, and blocked for 1 h in 10% FBS. Staining with specific mono- or polyclonal antibodies was done in 10% FBS with 0.5% saponin for 1 h. gal3 was immunostained using a specific mouse monoclonal anti-gal3 antibody (catalog no. 556904 [Transduction]; BD) at a 1:100 dilution. EEA-1 (Epit Mics) and LAMP-1 (Santa Cruz) were immunostained at 1:500 dilutions. Reovirus was immunostained using polyclonal reovirus antibody at a 1:200 dilution, and pVI was detected with rabbit polyclonal antiserum raised against purified preprotein VI (20) at a 1:1,000 dilution. Secondary Alexa Fluor 568-conjugated and DyLight 649-conjugated antibodies were used. Ad5gfp and *ts1* were prelabeled with Dylight 488 *N*-hydroxysuccinimide (NHS)-ester fluorophores (Thermo Scientific), according to the manufacturer's protocol prior to use. Hoechst stain from ImmunoChemistry Technologies or DAPI (4′,6′diamidino-2-phenylindole) was used to counterstain nuclei before coverslips were mounted on glass slides with ProLong Gold from Invitrogen. Z-stack images were acquired using identical parameters for each time point with a DeltaVision microscope (Applied Precision) and a CoolSnap HQ digital camera (Photometrics) with a 1.4-numerical aperture (NA) 100× objective lens and deconvolved with SoftWorx deconvolution software (Applied Precision). Images were assembled using IMARIS and ImageJ softwares. Virus particles and gal3 punctum three-dimensional surfaces were acquired using IMARIS software. Colocalization was determined by the fluorescence intensity of the protein of interest at each three-dimensional surface compared to the fluorescence intensity of the secondary-only control.

RESULTS

gal3 is recruited to punctate structures during Ad entry. Recently, gal3 was identified as a marker for vacuole lysis during bacterial infection (8, 25). gal3 is recruited to bacterially disrupted vacuole membranes by binding cell surface N-linked glycans exposed to the cytoplasm following membrane rupture (25). Binding of gal3 to membrane fragments can be visualized by immunofluorescence as punctate structures (8, 25). To determine whether Ad5 membrane penetration results in recruitment of gal3 to ruptured membranes, we infected HeLa cells with fluorescently labeled Ad5, and 30 min postinfection, the cells were fixed and stained for gal3. Analogous infections were performed with *ts1*, a temperature-sensitive mutant of Ad2 which, when virions are produced at the nonpermissive temperature, fails to disrupt endosomal membranes (7, 14, 33). In uninfected cells, gal3 is diffusely distributed in the cytoplasm and nucleus, with only rare puncta visible (Fig. 1A). Infection with Ad5 leads to the formation of multiple bright punctate gal3 structures (Fig. 1B). The diffuse staining seen in uninfected cells was also observed in cells infected with *ts1* (Fig. 1C). To determine whether this phenomenon could be used to distinguish between the modes of nonenveloped viral membrane penetration, these experiments were also performed with the reovirus type 3 Dearing strain (T3D; Fig. 1D), which forms pores in membranes rather than causing global membrane disruption as in the case of adenovirus (1, 18, 20). When we quantified the number of gal3 puncta per cell, we saw statistically significant differences in the numbers of puncta per cell in Ad5-infected cells compared to uninfected cells, *ts1*, and reovirus. These data suggest that gal3 is recruited to endosomal membranes disrupted during Ad5 entry.

If gal3 accumulates on disrupted endosomal membranes during Ad5 infection, we would expect that increasing the virus concentration should increase the number of disrupted endosomes and therefore increase the number of gal3 puncta observed. Thus, we infected HeLa cells with increasing multiplicities of infection (MOIs) of fluorescently labeled Ad5 and examined the correlation between the number of cell-associated virions and the number of gal3 puncta at 30 min postinfection by an immunofluorescence assay (IFA). Our data suggest that increasing the virus concentrations increased the number of gal3 puncta (Fig. 2). These observations are in agreement with the Ad5 MOI-dependent increases in the delivery of coendocytosed ribotoxins into the cytoplasm of cells (20).

Live-cell imaging of Ad5 membrane rupture and endosome escape. When imaging Ad5-induced gal3 puncta in fixed cells, we

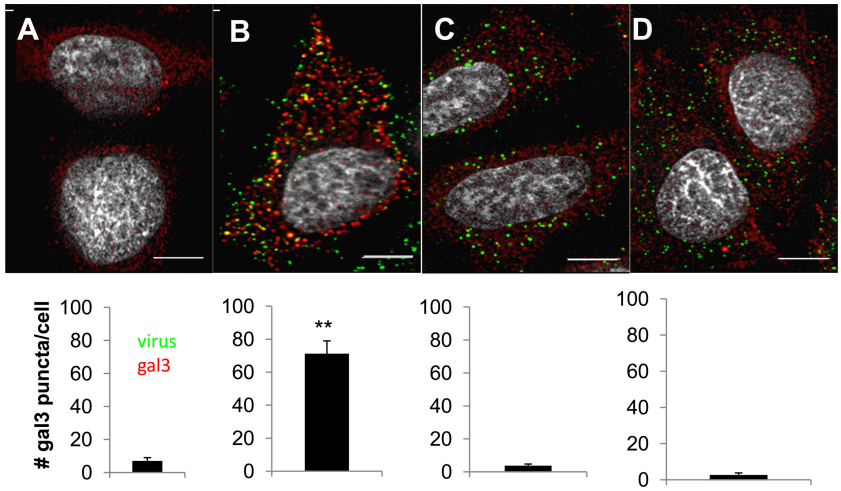

FIG 1 gal3 accumulates in punctate structures in Ad5-infected cells. HeLa cells were either left uninfected (A) or infected with fluorescently labeled (green) Ad5 (B), Ad2ts1 (C), or reovirus T3D (D), and at 30 min postinfection, the cells were fixed and stained for gal3 (red) or reovirus. The number of gal3 puncta per cell was counted. Bars, 5 μm. **, $P < 0.001$.

often observe Ad5 in gal3 punctate structures at or near the cell surface at early times postinfection (Fig. 3A). We confirmed that gal3 puncta correlate with release of pVI release by staining for gal3 and pVI in addition to the Alexa 488-labeled virions. Colocalization of both markers with labeled virions was observed at 30 min postwarming at, or very near, the cell surface (Fig. 3A, right panel).

To determine the kinetics of Ad5 membrane rupture and endosomal escape in real time, U2OS osteosarcoma cells, stably expressing mCherry-gal3, were infected with Alexa 488-labeled Ad5 and cells subjected to live-cell imaging. As seen by immunostaining for endogenous gal3, mCherry-gal3 appeared diffuse throughout the cytoplasm of uninfected cells (data not shown). Upon Ad5 infection, punctate gal3 fluorescence was observed. For technical reasons, we used asynchronous infections performed at 37°C without prebinding of virus. Using this approach, several impor-

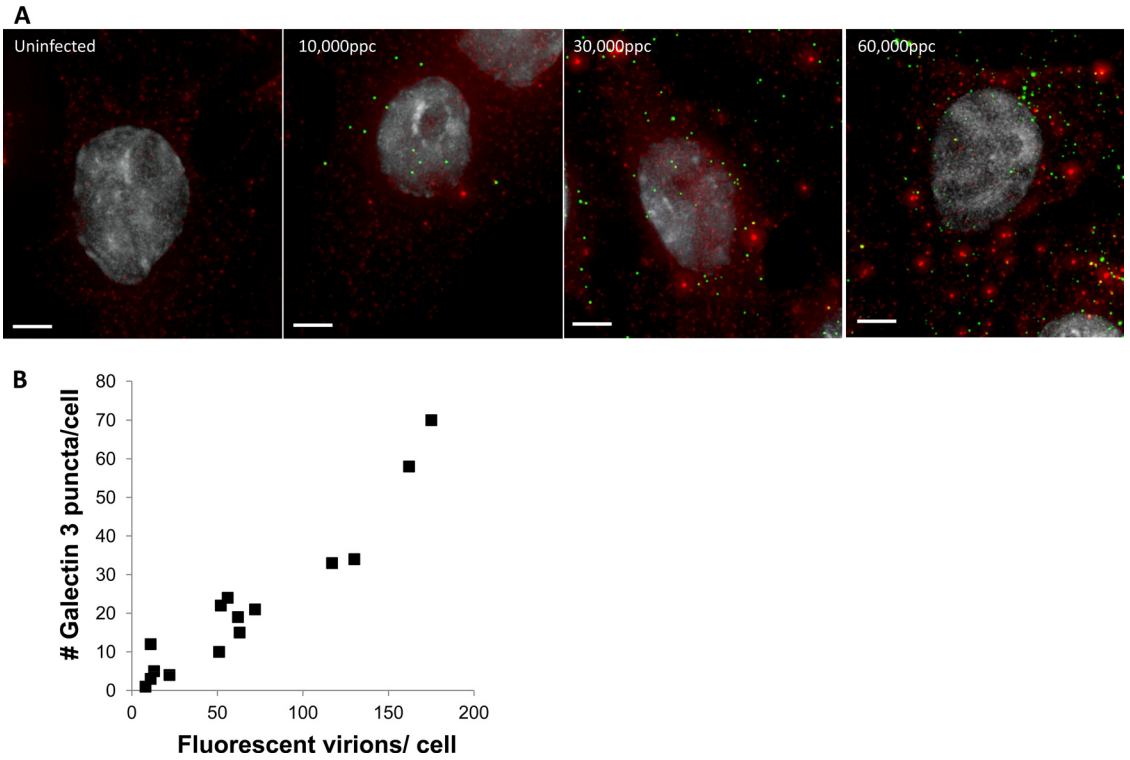

FIG 2 The number of gal3 puncta increases with increasing virus concentration. HeLa cells were infected with increasing concentrations of fluorescently labeled Ad5 (green). Cells were fixed and stained for gal3 (red) at 30 min postinfection. (A) Representative images. Bars, 5 μm. (B) The numbers of gal3 and virus puncta per cell were counted.

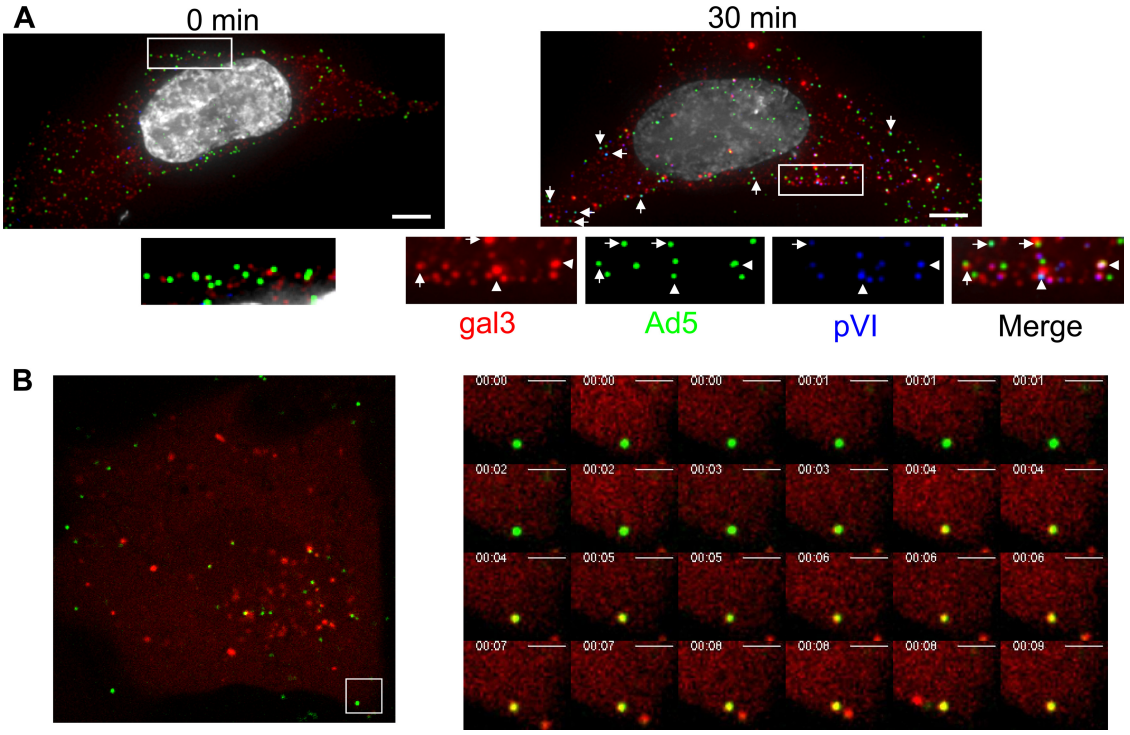

FIG 3 Ad5 membrane rupture occurring near the cell surface. (A) HeLa cells were infected with fluorescently labeled Ad5, fixed at 0 and 30 min postinfection, and stained for gal3 (red) and pVI (blue). Nuclei were stained with DAPI (gray). Bar, 5 μm. (B) U2OS cells stably expressing mCherry-gal3 were infected with Alexa 488-Ad5, and images were collected 15 min postinfection and collected at 5 Hz.

tant observations were made. First, recruitment of maximal mCherry-gal3 to Ad5-ruptured membranes was rapid, typically taking less than 1 s from the first observation of colocalization to maximal colocalization of all pixels attributed to a single virion (Fig. 3B; see also movie S1 in the supplemental material). Interestingly, colocalization of gal3 with Ad5, presumably representing ruptured endosomes, had a surprisingly long half-life, as many viruses remained colocalized with gal3 puncta for the duration of the movie (~320 s). This suggests that membrane rupture is temporally and spatially distinct from endosomal egress. It also suggests that pVI membrane rupture is not sufficient for the virus to escape from endosomes.

Using live-cell imaging of asynchronously infected cells, 30 min after addition of the virus, we also characterized endosomal egress events. As shown in Fig. 4, Ad5 was seen initially in gal3$^+$ endosomes which were predominantly perinuclear and relatively immobile. Whether these viruses trafficked to this perinuclear location in gal3$^+$ endosomes, and whether the endosomal membranes were already disrupted or resealed, is unknown. Upon egress, Ad5 underwent rapid directional movement, as indicated by traces (Fig. 4) in agreement with previous observations of microtubule-dependent movement of the virus in the cytoplasm (15, 30, 31). Further population-based analyses of the velocity and root mean square displacement of viruses within gal3$^+$ endosomes and upon endosomal egress could shed light on the state of adenovirus undergoing the classes of movement identified previously (6).

Exposure of pVI occurs prior to trafficking to EEA-1$^+$ early endosomes. Several lines of evidence suggest that Ad5 traffics through early endosomes prior to endosomal escape (12). More recent data suggest that species C Ads can uncoat and expose pVI at or near the cell surface, however (6, 34). To examine in more detail the compartmentalization of pVI release, we performed synchronous infections with fluorescently labeled Ad5 and stained for the early endosomal marker, EEA-1, as well as for pVI or gal3 at various times postinfection. We observed colocalization of Ad5 with pVI beginning at 10 min postinfection, with maximal colocalization occurring at 20 min postinfection (Fig. 5A). While 52% of Ad5 colocalized with pVI at 20 min postinfection, less than 25% of incoming Ad5 colocalized with both pVI and EEA-1. This suggests that exposure of pVI occurs prior to or outside early endosomes.

To determine whether gal3 recruitment to Ad5 occurs in a subset of endosomal compartments, analogous experiments were performed by immunostaining for gal3 and EEA-1 or LAMP-1, the late endosome/lysosome marker. Maximum colocalization of Ad5 with gal3 occurred 20 to 40 min postinfection (Fig. 5B). Less than half of the Ad5 that colocalized with gal3 also colocalized with EEA-1 (Fig. 5B). We propose that the majority of Ad5 virions do not rupture membranes in early endosomal compartments. It is even less likely that Ad5 ruptures membranes in late endosomes/lysosomes, as less than 2% of Ad5 colocalizing with gal3 also colocalized with the late endosome/lysosome marker LAMP-1 (Fig. 5C). Taken together, these data suggest that pVI exposure occurs prior to virus trafficking to early endosomes or in endosomal compartments not containing the common early and late endosomal markers EEA-1 and LAMP-1. Furthermore, fewer than half of the Ad5 membrane rupture events occurred in early endosomes or late endosomes/lysosomes, suggesting that the majority of virions rupture membranes at alternative sites.

Exposure of pVI precedes gal3 recruitment to endosomal membranes. The results of previous studies suggest that, during

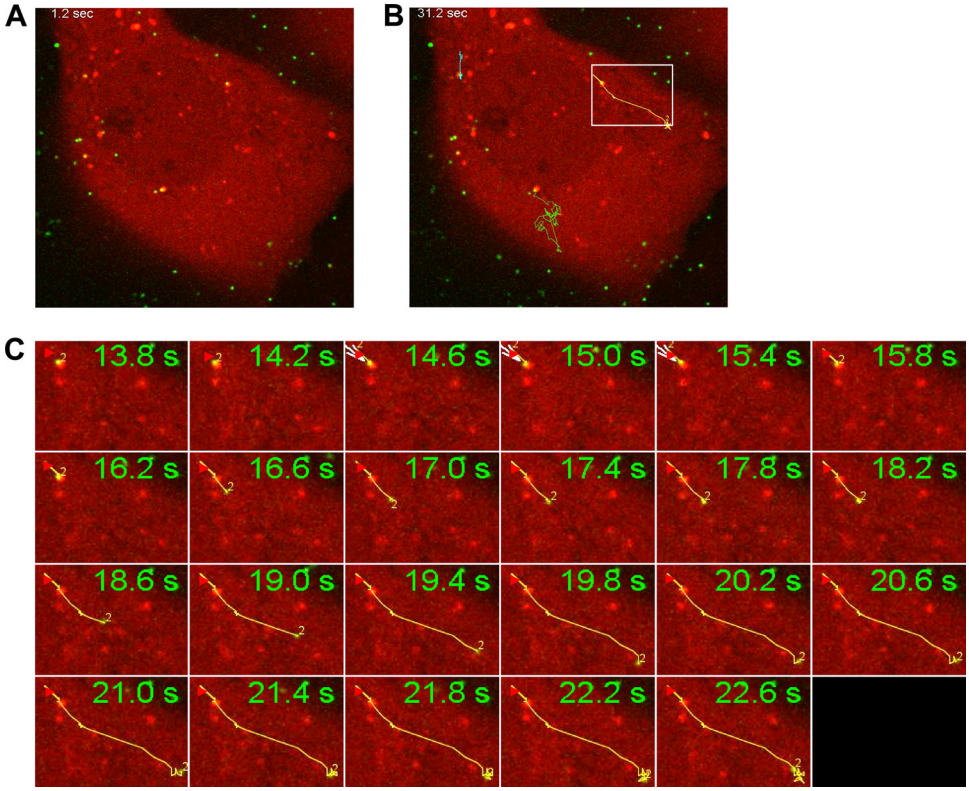

FIG 4 Time-resolved imaging of Alexa 488-Ad5 endosomal escape in U2OS cells expressing mCherry-gal3. Images were collected 30 min after infection at a rate of 5 Hz. (A) Frame showing cells prior to endosomal escape. (B) Traces tracking the movement of the fluorescent virions away from relatively immobile gal3$^+$ structures. (C) Montage showing the rapid directional movements of a fluorescent virion (from white box in panel B) as monitored by MTrackJ in ImageJ.

cell entry, pVI release from the capsid interior must occur for viral membrane penetration to take place (27, 33). To more carefully examine the correlation between kinetics of pVI release from the capsid interior and recruitment of gal3 to disrupted endosomal membranes, we examined a synchronous infection from virus binding to 4 h post-virus internalization, immunostaining for both pVI and gal3 in fixed cells. pVI release from the capsid interior is abundantly detected at 10 min post-virus internalization, consistent with published observations (Fig. 6A and B) (6, 34). gal3 recruitment to endosomal membranes is detected 20 min post-virus internalization, after pVI has already been released from the capsid (Fig. 6A and B). These data provide kinetic evidence that pVI release from the capsid interior precedes membrane rupture.

After endosomal escape, the partially disassembled virion traffics to the nuclear envelope to deliver its genome into the nucleus. We would therefore expect that, early during infection, when the virus disrupts the endosomal membrane, gal3 should colocalize with virus and pVI. As the virus escapes from endosomes, we would expect a decrease in gal3-virus colocalization. To test this, we used image analysis software to determine the percentage of gal3 that colocalizes with both virus and pVI, virus alone, pVI alone, or neither viral component at the different times post-virus internalization. When gal3 is recruited to endosomal membranes, 70% of gal3 puncta colocalize with virus, and this colocalization decreases to 50% by 1 h (Fig. 6C). These data are in agreement with viral escape from ruptured endosomes. While the colocalization of gal3 with virus decreases, the percentages of gal3$^+$ pVI$^+$ puncta remain similar at all time points, suggesting that it remains behind, associated with the endosomal membrane (Fig. 6C). Furthermore, we saw a maximal number of pVI and gal3 puncta per cell at 30 min which decreased by 1 h for both gal3 and pVI (Fig. 6B). Taken together, these data suggest that pVI release from virions precedes membrane rupture, as expected. Subsequently, following the recruitment of gal3 to ruptured membranes, virions separate from gal3, leaving pVI behind. The decrease in numbers of pVI and gal3 puncta at later times postinfection suggests that either gal3 and pVI dissociate from membranes or the disrupted membranes are somehow degraded after Ad5 escape.

DISCUSSION

Although numerous studies indirectly document a membranelytic event during Ad cell entry, visualizing virus rupture of endosomes and subsequent egress of the virus into the cytoplasm has been elusive. Electron-microscopic studies of Ad-infected cells have been able to capture the virus at the cell surface, in an intact endosome, or in the cytoplasm but have been unable to adequately describe Ad crossing a disrupted endosomal membrane (12, 17, 23). Our study identified gal3 as a marker for Ad rupture of endosomal membranes during cell entry. We have shown that gal3 can be used to demarcate events during Ad cell entry occurring prior to, during, or after endosomal membrane rupture, such as capsid uncoating, egress from ruptured endosomes, and intracellular trafficking. Furthermore, gal3 appears to be a useful tool for categorizing the mechanisms of membrane penetration used by nonenveloped viruses to cross cell membranes and is likely be useful in

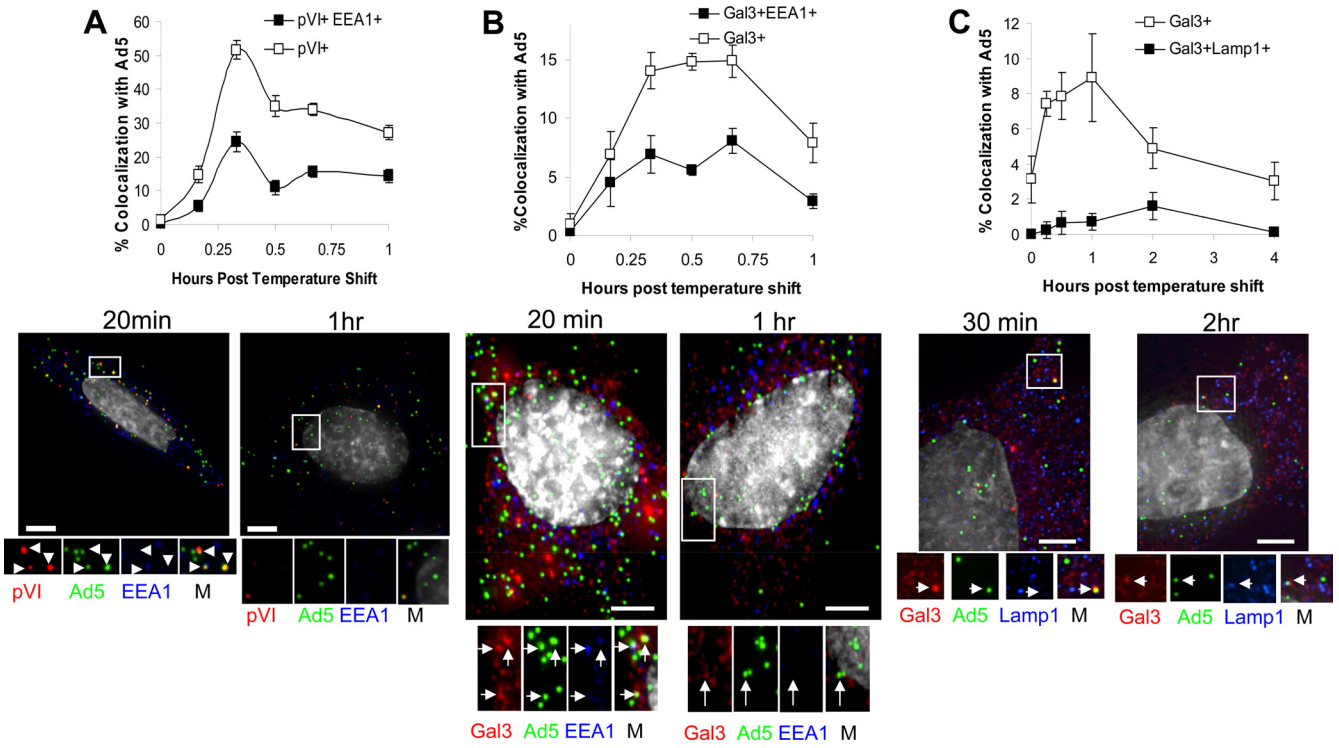

FIG 5 Ad5 acquires pVI and gal3 prior to early endosomes. Fluorescently labeled Ad5 (green) was bound to HeLa cells for 1 h at 4°C, after which cells were washed and shifted to 37°C. Cells were fixed and stained for gal3 (red) and pVI (A), EEA-1 (B), or LAMP-1 (C). M, merged images. The percentage of Ad5 colocalization was determined. Error bars indicate the standard error of the mean. Bars, 5 μm.

clarifying the specific contributions of viral and host proteins to adenovirus cell entry.

gal3 was first identified as a marker for vacuole lysis during bacterial infection (8, 25). Similar to what was observed during bacterial phagosomal lysis, we found that gal3 punctate structures formed very early in Ad5-infected cells (Fig. 1 and 4), were dependent on Ad endosomal membrane rupture, and could be visualized in real time. Interestingly, gal3 did not appear to be recruited to endosomes in cells following infection with the nonenveloped reovirus (Fig. 1). Unlike Ad5, which grossly reorganizes ruptured endosomal membranes, reovirus forms size-selective pores in membranes (1, 18). Given the diversity in subcellular localizations and potential methods used by other viruses such as polyomavirus, papillomavirus, parvoviruses, or rotaviruses, gal3 may be a useful tool to categorize the membrane penetration mechanisms of nonenveloped viruses.

Identifying a marker for disrupted endosomal membranes allowed us to ask questions about the kinetics and subcellular location of Ad membrane rupture and endosomal escape. Based on several previous reports, a model for Ad5 penetration of endosomal membranes has been proposed in which rupture of endosomal membranes occurs only after the capsid partially disassembles and pVI is released from the capsid interior (7, 15, 20, 22, 33). With a molecular marker to monitor Ad5 membrane rupture during cell entry, we found that this event occurred within 10 min of the initial detection of pVI release from the capsid interior (Fig. 5 and 6). When these gal3-positive membranes are first detected ~20 min postinfection, they colocalize with both virus and pVI (Fig. 2 and 6), and we suggest that they represent a virion associated with ruptured membranes. Live-cell imaging of this event demonstrates that viral mobility increases substantially after egress from gal3-positive endosomes, which may reflect previous observations that Ad5 moves along microtubules once in the cytoplasm (5, 30).

Previously, the Ad lytic event has been measured as the translocation of membrane-impermeative ribotoxins (22, 33, 34) and antibody-toxin conjugates (10) across the endosomal membrane. By infecting cells overexpressing mCherry-gal3 with fluorescently labeled Ad5, we were able to visualize Ad rupturing membranes in real time. Preliminary data suggest that recruitment of gal3 occurs rapidly, in under a second (Fig. 3A). However, based on the analysis of the kinetics of gal3 recruitment to Ad5-ruptured membranes by immunostaining for endogenous gal3 in fixed cells, it appears that the time at which gal3 is recruited to membranes is somewhat heterogeneous. Interestingly, the virus appears to remain associated with ruptured endosomes for upward of several minutes, as evidenced by colocalization of virus with gal3. At later times postinfection, Ad5 in gal3$^+$ structures appears largely static, although longer-range motions are apparent in some cases (Movie S2 in the supplemental material and data not shown). But with observations of gal3 recruitment to Ad5 near the cell surface and egress from endosomes occurring primarily from perinuclear locations, future experiments are planned to more carefully quantify whether Ad5 is moving between these two sites in gal3$^+$ structures. While data from fixed-cell images of Ad5-infected HeLa cells demonstrate Ad5 rupture of membranes at or near the cell surface similar to what is observed by live-cell imaging of Ad5 infection in U2OS cells, we cannot rule out the possibility that the sites of endosomal egress differ between these two cell types. While U2OS cells, used for live-cell imaging, have levels of CAR protein

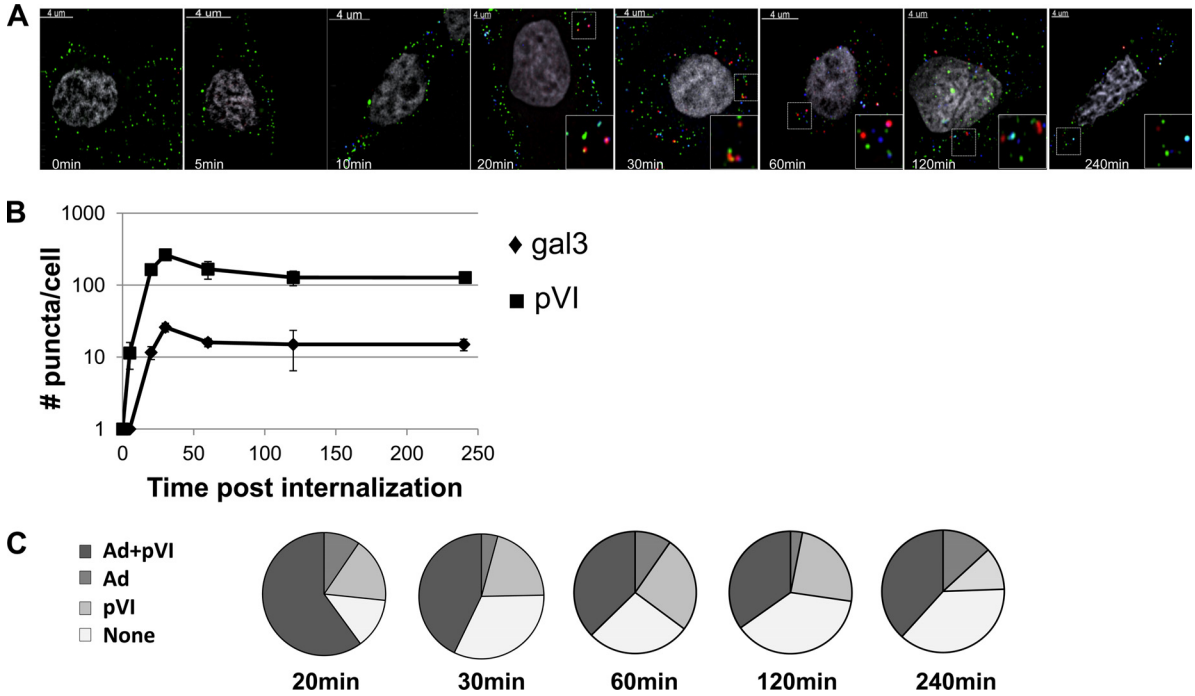

FIG 6 Ad5-pVI exposure precedes gal3 recruitment. Fluorescently labeled Ad5 (green) was bound to HeLa cells for 1 h, after which the cells were washed and shifted to 37°C to allow virus internalization. (A) Cells were fixed and stained for pVI (blue) and gal3 (red) at different times post-virus internalization. Inserts represent enlarged views of gal3 puncta. (B) The numbers of gal3 and pVI puncta per cell were counted for each time point. Error bars indicate the standard error of the mean. (C) The percentages of gal3 puncta colocalizing with Ad5, pVI, or both or with gal3 alone (None) at the indicated time points were determined.

expression similar to those seen with HeLa cells (13), the integrin levels of these two cell lines have not been directly compared. Differences in integrin expression could influence Ad trafficking and the kinetics of endosomal escape.

While it is unclear whether Ad5 movement occurs in gal3$^+$ structures where the membranes remain ruptured or whether the membrane has resealed, we do see that Ad5 can escape from these gal3 punctate structures. Once the virus is able to break free from these endosomes, the velocity and distance of viral movements appear to be significantly increased in most cases. The remnants of the ruptured endosome seen after Ad5 breaks free appear to remain relatively immobile, however. This apparent struggle of Ad5 to dissociate from ruptured endosomes is intriguing. Whether this delay between endosomal rupture and viral egress from endosomes is related to the kinetics of release of pVI from the capsid interior, the need to recruit additional host factors to ruptured endosomal membranes to facilitate viral escape into the cytoplasm, or some combination of these occurrences is the subject of ongoing investigations.

The fate of gal3$^+$ pVI$^+$ membranes after viral escape from endosomes remains unknown. Our data indicate that the total number of pVI$^+$ and gal3$^+$ structures decreases significantly after peaking 0.5 to 1 h post-virus internalization. This is in agreement with previous reports suggesting that pVI is degraded after dissociation from the viral capsid (15). Although the total number of gal3$^+$ and pVI$^+$ membrane remnants decreases at later times postinfection, the percentage of gal3 that colocalizes with pVI remains relatively constant. These data suggest that, after endosomal membrane rupture, gal3/pVI-decorated remnants of ruptured endosomes are targeted for degradation. Previous reports have suggested that phagosomal membrane remnants generated during bacterial rupture are sequestered by autophagy and degraded within lysosomes (8). Although degradation of pVI during cell entry was previously proposed to be mediated by the virally encoded 23K cysteine protease (14), the fact that pVI appears to remain associated with gal3-positive membrane remnants after Ad5 endosomal escape suggests that pVI could be degraded by an alternative mechanism. Given the potential membrane-damaging effects of pVI remaining in cells after Ad5 membrane penetration, further studies of the fate of pVI after Ad5 endosomal escape are warranted.

In addition to answering questions regarding the mechanism used by Ad to rupture membranes, our results have allowed us to better define the endosomal compartment from which Ad escapes. Ad type 2 was shown to traffic to the early endosomal compartment, as visualized by colocalization with the early endosomal marker EEA-1 (12), and is found less frequently in late endosomes or lysosomes (12). Our data suggest that release of pVI from the capsid interior occurs early after infection, perhaps before early endosomes are encountered (Fig. 5A). These observations are in agreement with those of others, who have suggested that pVI is exposed as early as at the cell surface (6, 34). Further, while we observed localization of Ad5 with EEA-1$^+$ endosomes similar to that previously reported by other groups (22), the majority of gal3 recruitment to Ad5 occurred before Ad5 colocalized with early endosome (EEA-1) and late endosome/lysosome (LAMP-1) markers (Fig. 5). Together, these data suggest either that Ad5 uncoats and ruptures membranes prior to reaching early endosomal compartments or that Ad5 membrane rupture occurs within an endosomal compartment, induced or otherwise, which does not

traffic through early endosomes/late endosomes/lysosomes. Given observations of Ad5 membrane rupture near the cell surface and escape from endosomes located in a perinuclear compartment, these data suggest that Ad5 may use a novel endosomal trafficking route to efficiently enter cells. Alternatively, incoming Ad5 virions in ruptured endosomes could be in an EEA-negative endosomal compartment that would eventually become EEA positive, which cannot be captured using fixed-cell imaging. Since a potential caveat to this, and to all microscopy studies of virus trafficking, arises from uncertainty in determining definitively whether the trafficking of an imaged virion leads to productive infection, further studies are clearly needed to better define the location of Ad5 uncoating and rupture of host cell membranes.

Overall, the use of gal3 as a marker for Ad5 endosomal escape has allowed us to further define key events in Ad cell entry occurring before, during, and after endosomal membrane rupture. This marker is likely to serve as a unique tool to characterize the membrane penetration events of other nonenveloped viruses. Ultimately, gal3 recruitment to virus-ruptured membranes provides a unique opportunity to better understand how nonenveloped viruses penetrate cell membranes.

ACKNOWLEDGMENTS

This work was supported by the American Heart Association (2261306 to C.M.W.), the National Institute of Allergy and Infectious Diseases (AI082430 to C.M.W. and AI007508 to S.A.M.), and FRM Equipe 2011 grant DEQ 20110421299 (H.W.).

We acknowledge Christel Pujol and the Bordeaux imaging center (BIC) for help setting up the live-cell imaging acquisition. Pranav Danthi (Indiana U.) kindly provided reovirus and reagents.

REFERENCES

1. **Agosto MA, Ivanovic T, Nibert ML.** 2006. Mammalian reovirus, a nonfusogenic nonenveloped virus, forms size-selective pores in a model membrane. Proc. Natl. Acad. Sci. U. S. A. **103**:16496–16501.
2. **Barlan AU, Danthi P, Wiethoff CM.** 2011. Lysosomal localization and mechanism of membrane penetration influence nonenveloped virus activation of the NLRP3 inflammasome. Virology **412**:306–314.
3. **Barlan AU, Griffin TM, McGuire KA, Wiethoff CM.** 2011. Adenovirus membrane penetration activates the NLRP3 inflammasome. J. Virol. **85**:146–155.
4. **Barondes SH, et al.** 1994. Galectins: a family of animal beta-galactoside-binding lectins. Cell **76**:597–598.
5. **Bremner KH, et al.** 2009. Adenovirus transport via direct interaction of cytoplasmic dynein with the viral capsid hexon subunit. Cell Host Microbe **6**:523–535.
6. **Burckhardt CJ, et al.** 2011. Drifting motions of the adenovirus receptor CAR and immobile integrins initiate virus uncoating and membrane lytic protein exposure. Cell Host Microbe **10**:105–117.
7. **Cotten M, Weber JM.** 1995. The adenovirus protease is required for virus entry into host cells. Virology **213**:494–502.
8. **Dupont N, et al.** 2009. Shigella phagocytic vacuolar membrane remnants participate in the cellular response to pathogen invasion and are regulated by autophagy. Cell Host Microbe **6**:137–149.
9. **Farr GA, Zhang LG, Tattersall P.** 2005. Parvoviral virions deploy a capsid-tethered lipolytic enzyme to breach the endosomal membrane during cell entry. Proc. Natl. Acad. Sci. U. S. A. **102**:17148–17153.
10. **FitzGerald DJ, Padmanabhan R, Pastan I, Willingham MC.** 1983. Adenovirus-induced release of epidermal growth factor and pseudomonas toxin into the cytosol of KB cells during receptor-mediated endocytosis. Cell **32**:607–617.
11. **Furlong DB, Nibert ML, Fields BN.** 1988. Sigma 1 protein of mammalian reoviruses extends from the surfaces of viral particles. J. Virol. **62**:246–256.
12. **Gastaldelli M, et al.** 2008. Infectious adenovirus type 2 transport through early but not late endosomes. Traffic **9**:2265–2278.
13. **Graat HC, et al.** 2005. Coxsackievirus and adenovirus receptor expression on primary osteosarcoma specimens and implications for gene therapy with recombinant adenoviruses. Clin. Cancer Res. **11**:2445–2447; author reply, **11**:2447–2448.
14. **Greber UF, Webster P, Weber J, Helenius A.** 1996. The role of the adenovirus protease on virus entry into cells. EMBO J. **15**:1766–1777.
15. **Greber UF, Willetts M, Webster P, Helenius A.** 1993. Stepwise dismantling of adenovirus 2 during entry into cells. Cell **75**:477–486.
16. **Houzelstein D, et al.** 2004. Phylogenetic analysis of the vertebrate galectin family. Mol. Biol. Evol. **21**:1177–1187.
17. **Imelli N, Ruzsics Z, Puntener D, Gastaldelli M, Greber UF.** 2009. Genetic reconstitution of the human adenovirus type 2 temperature-sensitive 1 mutant defective in endosomal escape. Virol. J. **6**:174.
18. **Ivanovic T, et al.** 2008. Peptides released from reovirus outer capsid form membrane pores that recruit virus particles. EMBO J. **27**:1289–1298.
19. **Leffler H, Carlsson S, Hedlund M, Qian Y, Poirier F.** 2004. Introduction to galectins. Glycoconj. J. **19**:433–440.
20. **Maier O, Galan DL, Wodrich H, Wiethoff CM.** 2010. An N-terminal domain of adenovirus protein VI fragments membranes by inducing positive membrane curvature. Virology **402**:11–19.
21. **McGuire KA, Barlan AU, Griffin TM, Wiethoff CM.** 2011. Adenovirus type 5 rupture of lysosomes leads to cathepsin B-dependent mitochondrial stress and production of reactive oxygen species. J. Virol. **85**:10806–10813.
22. **Moyer CL, Wiethoff CM, Maier O, Smith JG, Nemerow GR.** 2011. Functional genetic and biophysical analyses of membrane disruption by human adenovirus. J. Virol. **85**:2631–2641.
23. **Nakano MY, Boucke K, Suomalainen M, Stidwill RP, Greber UF.** 2000. The first step of adenovirus type 2 disassembly occurs at the cell surface, independently of endocytosis and escape to the cytosol. J. Virol. **74**:7085–7095.
24. **Nemerow GR, Stewart PL.** 1999. Role of alpha(v) integrins in adenovirus cell entry and gene delivery. Microbiol. Mol. Biol. Rev. **63**:725–734.
25. **Paz I, et al.** 2010. Galectin-3, a marker for vacuole lysis by invasive pathogens. Cell Microbiol. **12**:530–544.
26. **Prchla E, Plank C, Wagner E, Blaas D, Fuchs R.** 1995. Virus-mediated release of endosomal content in vitro: different behavior of adenovirus and rhinovirus serotype 2. J. Cell Biol. **131**:111–123.
27. **Smith JG, Nemerow GR.** 2008. Mechanism of adenovirus neutralization by Human alpha-defensins. Cell Host Microbe **3**:11–19.
28. **Smith JG, et al.** 2010. Insight into the mechanisms of adenovirus capsid disassembly from studies of defensin neutralization. PLoS Pathog. **6**:e1000959. doi:10.1371/journal.ppat.1000959.
29. **Smith JG, Wiethoff CM, Stewart PL, Nemerow GR.** 2010. Adenovirus. Curr. Top. Microbiol. Immunol. **343**:195–224.
30. **Strunze S, et al.** 2011. Kinesin-1-mediated capsid disassembly and disruption of the nuclear pore complex promote virus infection. Cell Host Microbe **10**:210–223.
31. **Suomalainen M, Nakano MY, Boucke K, Keller S, Greber UF.** 2001. Adenovirus-activated PKA and p38/MAPK pathways boost microtubule-mediated nuclear targeting of virus. EMBO J. **20**:1310–1319.
32. **Weber J.** 1976. Genetic analysis of adenovirus type 2 III. Temperature sensitivity of processing viral proteins. J. Virol. **17**:462–471.
33. **Wiethoff CM, Wodrich H, Gerace L, Nemerow GR.** 2005. Adenovirus protein VI mediates membrane disruption following capsid disassembly. J. Virol. **79**:1992–2000.
34. **Wodrich H, et al.** 2010. A capsid-encoded PPxY-motif facilitates adenovirus entry. PLoS Pathog. **6**:e1000808. doi:10.1371/journal.ppat.1000808.